Chapter 6

Neural Networks as a Function Approximator in Generic Model Control

In this chapter the multilayer feedforward network is used as a function approximator in Generic Model Control (GMC). The objective is to control the temperature of the simulated Continuous Stirred Tank Reactor (CSTR) by manipulating the coolant feed temperature. The use of neural network technique and the GMC is a hybrid method proposed to improve the control performance of GMC.

6.1 Introduction

Generic Model Control (GMC), one of advanced control concepts, is a model-based control strategy which is not only a simple method but also easy to implement in control system. It can directly use nonlinear models of a process to determine a control action. Thus the nonlinear models do not need to be linearized. This control strategy has been studied by Lee and Sullivan (1988), Kittisupakorn and Kershenbaum (1994), Kershenbaum and Kittisupakorn (1994).

Reactor temperature control is very important as it affects the product quality and process operation. In this work, Generic Model Control (GMC) is utilised to control the reactor temperature of the continuous stirred tank reactor (CSTR) by manipulating coolant temperature. In the aspect of robustness, whether the GMC can handle a system in the presence of plant-model mismatch or not still depends on case by case. Hence

neural networks which have excellent nonlinear representational capabilities are employed with the GMC, as a hybrid method, to improve the control performance of the GMC either when some state variables cannot be measured online or when plant/model mismatch exists. The objective of this work is to investigate the GMC performance for the temperature control of the CSTR in a nominal case as well as in the presence of plant-model mismatches.

6.2 Generic Model Control Formulation

Generic Model Control (GMC) is a model-based control strategy which uses linear/nonlinear models of a system to compute a control action. A desired response can be obtained via two tuning parameters. Since the GMC can directly use nonlinear models of a process to determine a control action, the nonlinear models do not need to be linearized. Its application is however limited to systems which are linear in control.

The GMC controller design is based on the following model

$$\frac{dx}{dt} = f(x,d,t) + g(x,t)u \tag{6.1}$$

$$y = h(x) \tag{6.2}$$

where f, g, and h are nonlinear functions, x is the state of the system, y is the output, d is the disturbance, and u is the manipulated variable. The derivative of y is assumed to be given by a PI model as

$$\frac{dy}{dt} = K_1(y_{sp} - y) + K_2 \int_0^{t_f} (y_{sp} - y)dt \tag{6.3}$$

The K_1 and K_2 parameters can be varied to change the controller 's response. The method used to tune the parameter was presented by Lee and Sullivan (1988) (see Appendix D). Eq. (6.3) forces y toward its set point, y_{sp}, with zero offset. If Eq. (6.2) is

differentiated and together with Eq. (6.3) is substituted into Eq. (6.1), the following control law results

$$u = \frac{\left[K_1(y_{sp} - y) + K_2 \int (y_{sp} - y)dt - \frac{dh}{dx} f(x,d,t)\right]}{\left(\frac{dh}{dt} g(x,t)\right)} \tag{6.4}$$

Although the GMC has many advantages as described above, it still requires reasonable process models and parameters and measurement of controlled variables. Neural network (NN) is a powerful tool that can learn highly nonlinear models and therefore it is proposed to improve the GMC performance under the limitation above.

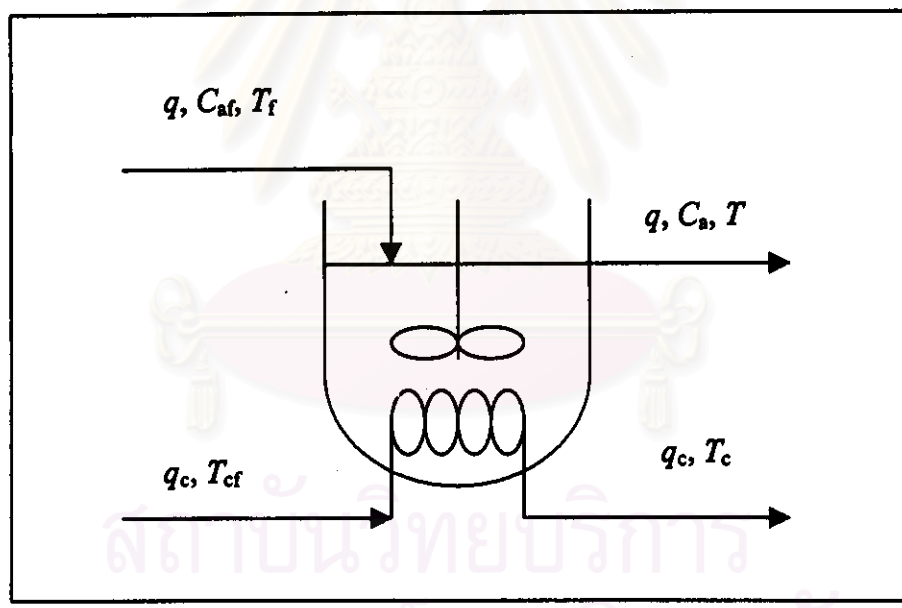

Figure 6.1: A schematic of continuous stirred tank reactor.

6.3 Continuous Stirred Tank Reactor

A schematic of the CSTR system is shown in Figure 6.1. A single irreversible, exothermic reaction A→B is assumed to occur in the reactor. The process model consists of two nonlinear ordinary differential equations (Henson and Seborg, 1990),

$$\frac{dC_A}{dt} = \frac{q}{v}(C_{Af} - C_A) - k_0 C_A \exp\left(-\frac{E}{RT}\right) \tag{6.5}$$

$$\frac{dT}{dt} = \frac{q}{V}(T_f - T) + \frac{(-\Delta H)k_0 C_A}{\rho C_p}\exp\left(-\frac{E}{RT}\right) + \frac{\rho_c C_{pc}}{\rho C_p V} q_c \left[1 - \exp\left(-\frac{hA}{q_c \rho_c C_{pc}}\right)\right](T_{cf} - T) \tag{6.6}$$

where C_A is the effluent concentration of component A, T is the reactor temperature, q is the feed flow rate and q_c is the coolant flow rate. The other model parameters are defined in the Nomenclature and the nominal operating is given in Table 6.1. For these conditions, there are three (two stable and one unstable) steady states. The operating point in Table 6.1 corresponds to the lower stable steady state. The objective is to control T by manipulating T_{cf}. Open-loop responses for +/- 15% step changes in T_{cf} are shown in Figure 6.2. It can be seen that for these step changes, the CSTR exhibits nonlinear dynamic behavior.

Table 6.1: Nominal operating condition of the continuous stirred tank reactor

$q = 100\,\mathrm{l\,min^{-1}}$	$E/R = 9.95\times10^{3}\,\mathrm{K}$
$C_{Af} = 1\,\mathrm{mol\,l^{-1}}$	$-\Delta H = 2\times10^{5}\,\mathrm{cal\,mol^{-1}}$
$T_f = 350\,\mathrm{K}$	$\rho, \rho_C = 1000\,\mathrm{g\,l^{-1}}$
$T_{Cf} = 350\,\mathrm{K}$	$C_p, C_{pC} = 1\,\mathrm{cal\,g^{-1}K^{-1}}$
$V = 100\ 1$	$q_C = 103.41\ 1\,\mathrm{min^{-1}}$
$hA = 7\times10^{5}\,\mathrm{cal\,min^{-1}K^{-1}}$	$T = 440.2\,\mathrm{K}$
$k_o = 7.2\times10^{10}\,\mathrm{min^{-1}}$	$C_A = 8.36\times10^{-2}\,\mathrm{mol\,l^{-1}}$

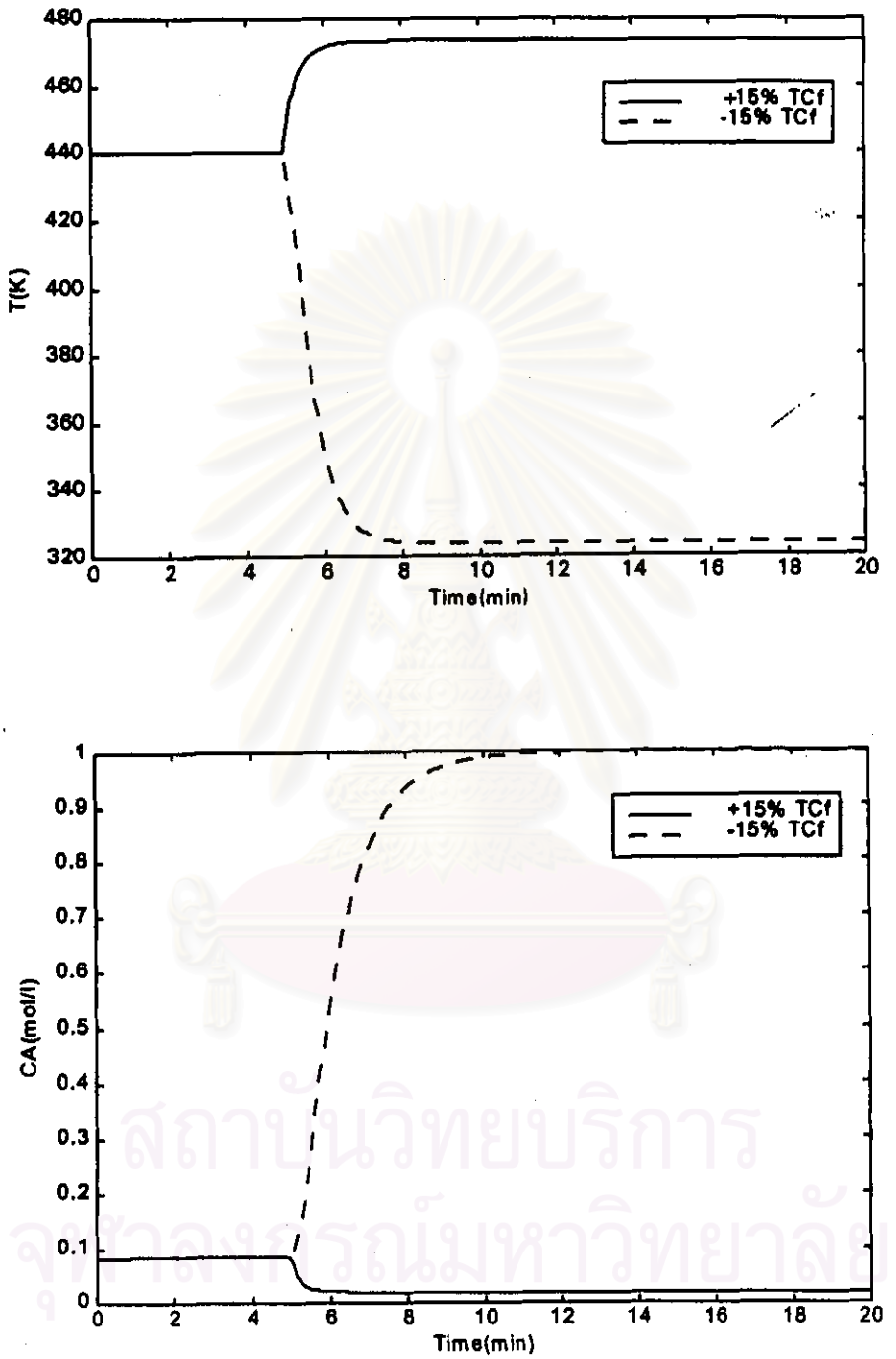

Figure 6.2: Open-loop response of CSTR for +/-15% change of coolant temperature. Reactor temperature (upper) and Effluent concentration of reactant A (lower)

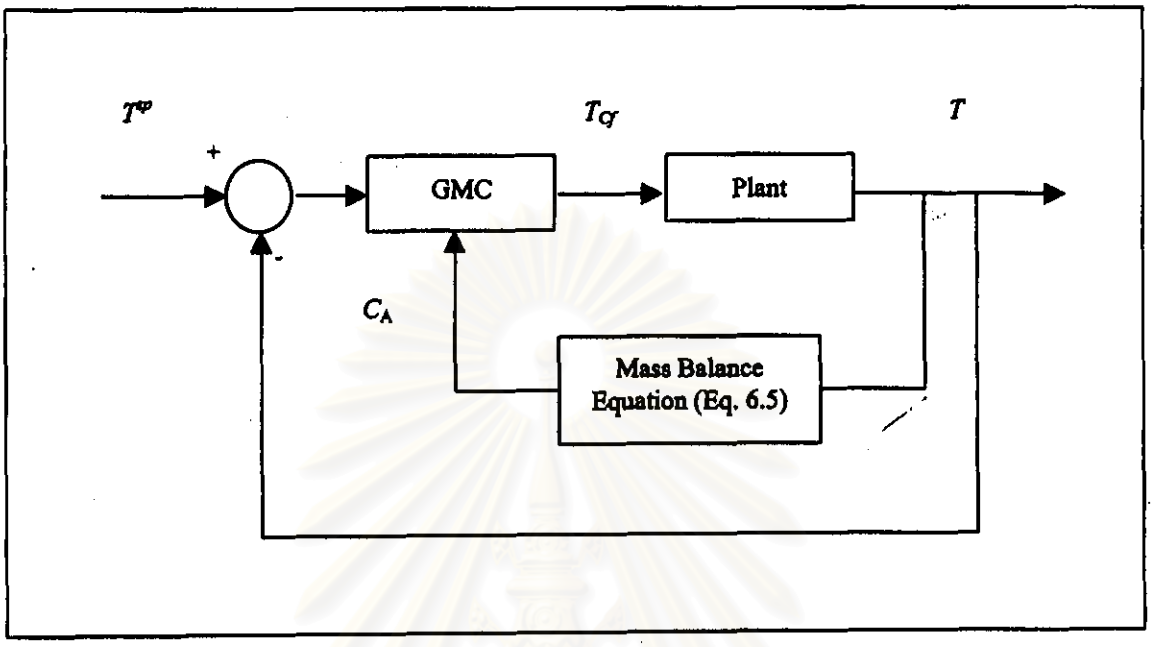

Figure 6.3: GMC configuration with an estimator.

For the CSTR studied, the following *f*, *g*, and *h* functions can be defined from the system model, Eq. (6.6)

$$f(x,d,t)=\frac{q}{V}(T_f-T)+\frac{(-\Delta H)k_oC_A}{\rho C_p}\exp\left(-\frac{E}{RT}\right) - \frac{\rho_c C_{pc} q_c}{\rho C_p V}\left[1-\exp\left(-\frac{hA}{q_c\rho_c C_{pc}}\right)\right]T \tag{6.7}$$

$$g(x,t)=\frac{\rho_c C_{pc} q_c}{\rho C_p V}\left[1-\exp\left(-\frac{hA}{q_c\rho_c C_{pc}}\right)\right] \tag{6.8}$$

$$h(x)=T \tag{6.9}$$

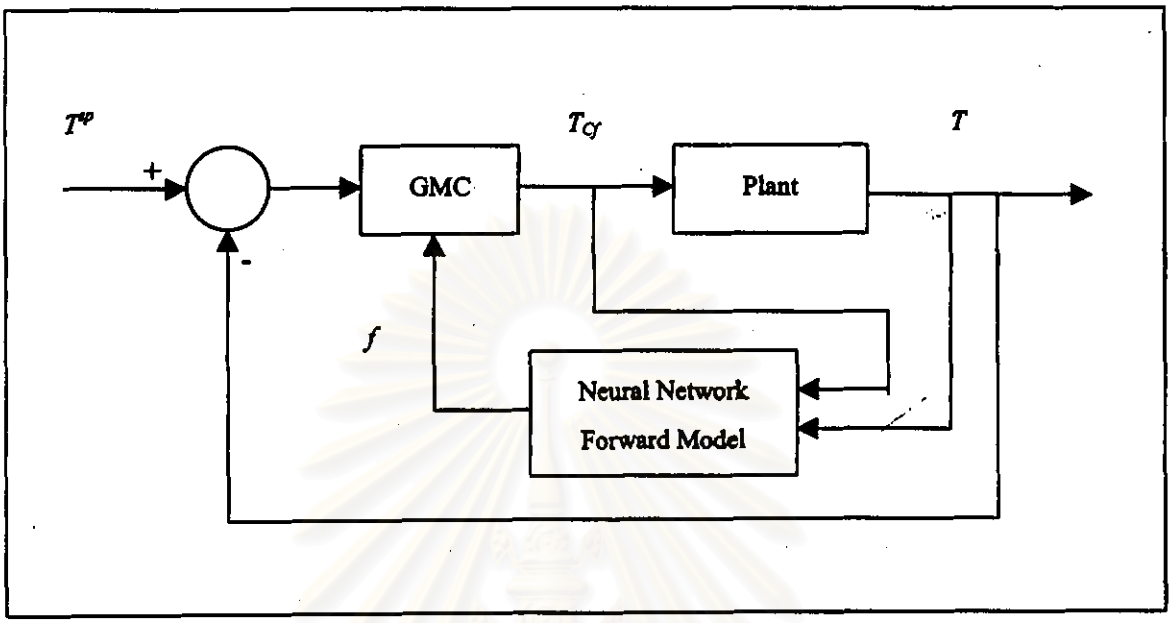

Figure 6.4: The network implementation in GMC configuration.

As can be seen from Eq. (6.7), f depends on both the effluent concentration of the reactant (C_A) and the reactor temperature (T) but only the reactor temperature is available online. Consequently, one method utilized to solve this problem is the estimation of unmeasured concentration from measured temperature using mass balance equation. Figure 6.3 shows the schematic of the GMC control with an estimator simulated from the mass balance equation. The other method is that neural network was utilized to predict the current value of f given the coolant and the reactor temperature. Because the CSTR is a single-input single output (SISO) system and the neural network model is trained offline, Levenberg-Marquardt algorithm being the fast training method is utilized. The sum-squared error is the criterion used to select the suitable neural network model for function approximation. The selected neural network structure consists of three input nodes (one current value of the coolant temperature and two past values of the reactor temperature), seven hidden nodes and one output node. The implementation of the neural network approximator in the GMC configuration is illustrated in Figure 6.4 and the neural network structure representing the function approximation is depicted in Figure 6.5.

Table 6.2: Performance and robustness tests on the GMC with mass balance estimator (GMC) and the GMC with neural network approximator (GMC-NN)

Performance Tests	Robustness Tests
1. Disturbance Rejection 1.1 10% T_f 1.2 10% C_{Af} 2. Set point Tracking T_{sp}: 440.2 K → 450 K	1.Nominal Condition 2.Plant-model mismatches 2.1 20% k_o 2.2 -50% hA 2.3 10% ($-\Delta H$)
Total	$3 \times 4 = 12$ case studies

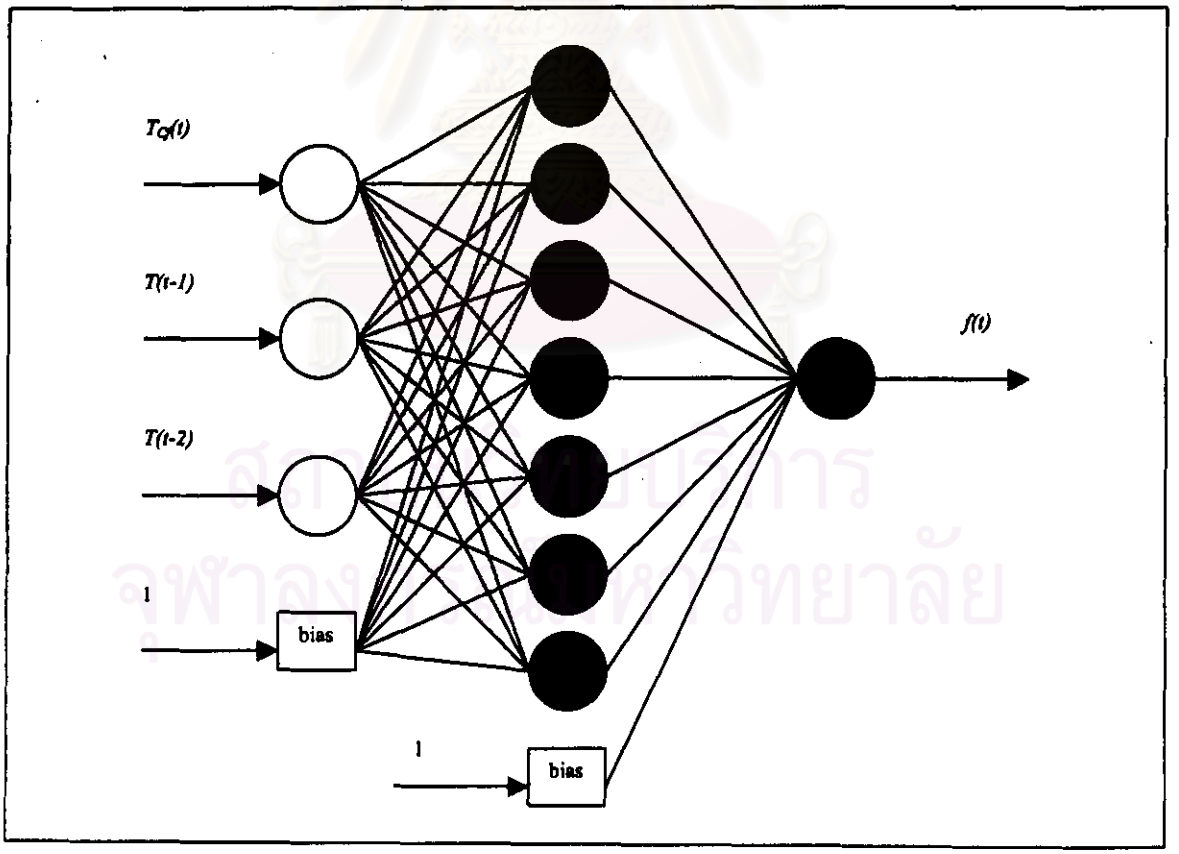

Figure 6.5: Neural network structure representing function approximator.

Table 6.3: Comparison of the GMC and the GMC-NN control performance

Robustness Tests	Performance Tests	IAE	
		GMC	GMC-NN
Nominal condition			
1. no change in parameters	10% T_f	0.0114	1.3165
2. no change in parameters	10%C_{Af}	18.3347	0.6342
Plant-model mismatches			
3. 20%*ko*	10% T_f	30.9862	1.5472
4. 20%*ko*	10% C_{Af}	21.1781	0.7442
5. –50%*hA*	10% T_f	14.9082	2.4230
6. –50%*hA*	10% C_{Af}	33.2395	1.4328
7. 10%*(-ΔH)*	10% T_f	18.3345	3.4525
8. 10%*(-ΔH)*	10% C_{Af}	38.4990	1.4743
Nominal condition			
9. no change in parameters	change T^{sp} to 450K	7.2814	7.1156
Plant-model mismatches			
10. 20%*ko*	change T^{sp} to 450K	34.1699	7.1266
11. –50%*hA*	change T^{sp} to 450K	18.9601	6.1852
12. 10%*(-ΔH)*	change T^{sp} to 450K	22.1832	6.2646

Note: Integral absolute error,

$$IAE = \int |e| dt$$

where $e = T^{sp} - T$

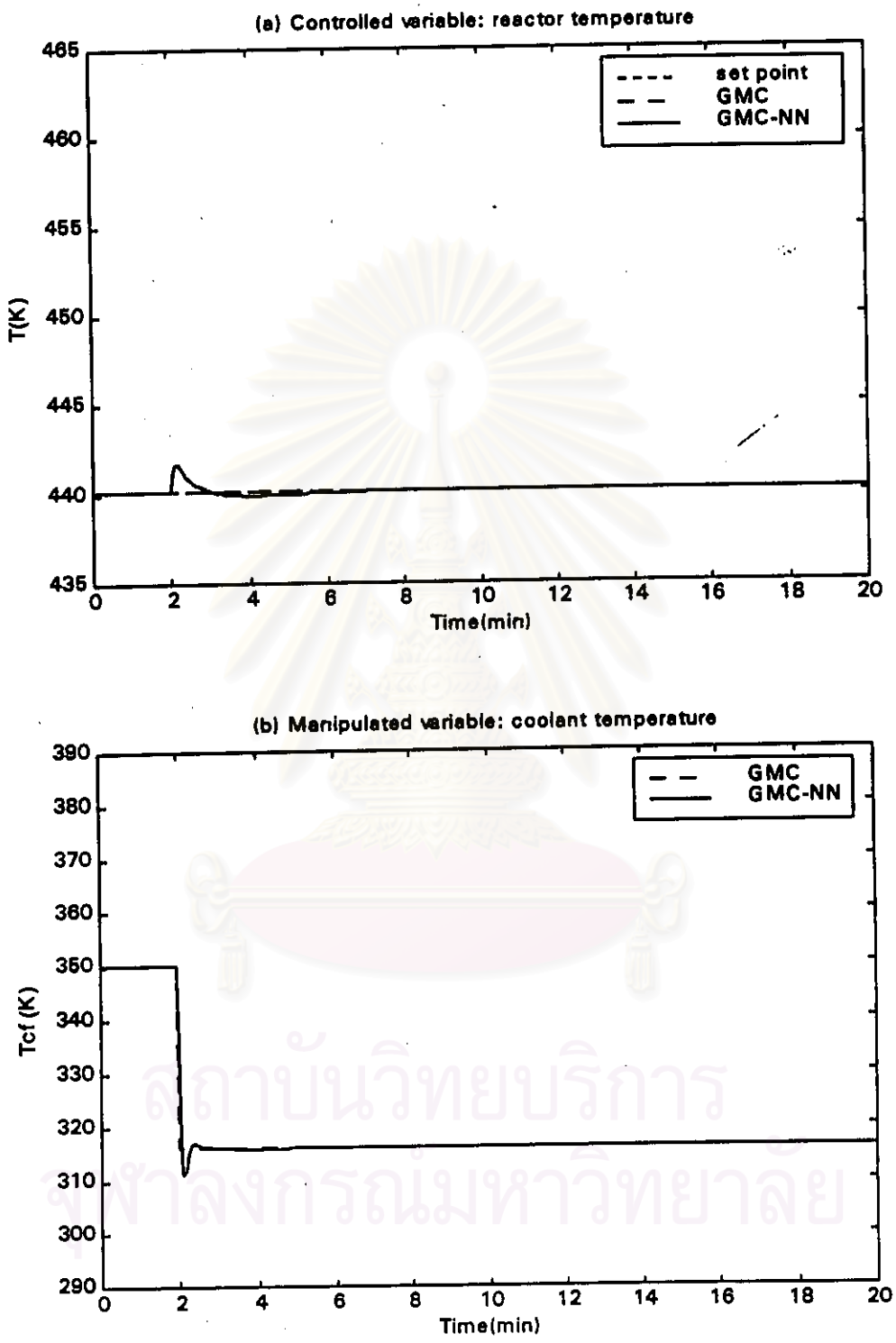

Figure 6.6: Disturbance rejection test with GMC and GMC-NN.
Response to 10% load disturbance in the measured feed temperature

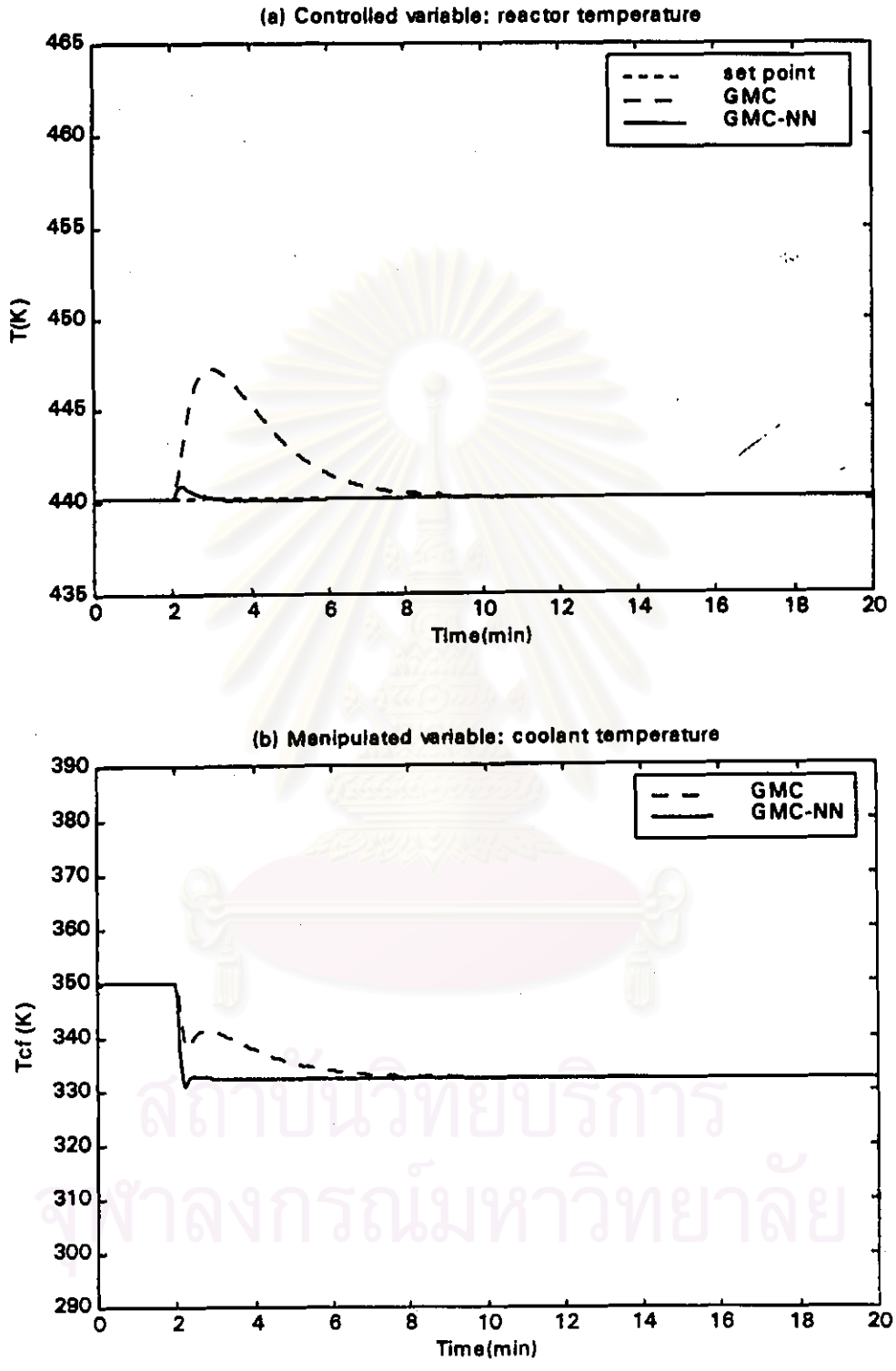

Figure 6.7: Disturbance rejection test with GMC and GMC-NN.
Response to 10% load disturbance in the unmeasured feed concentration

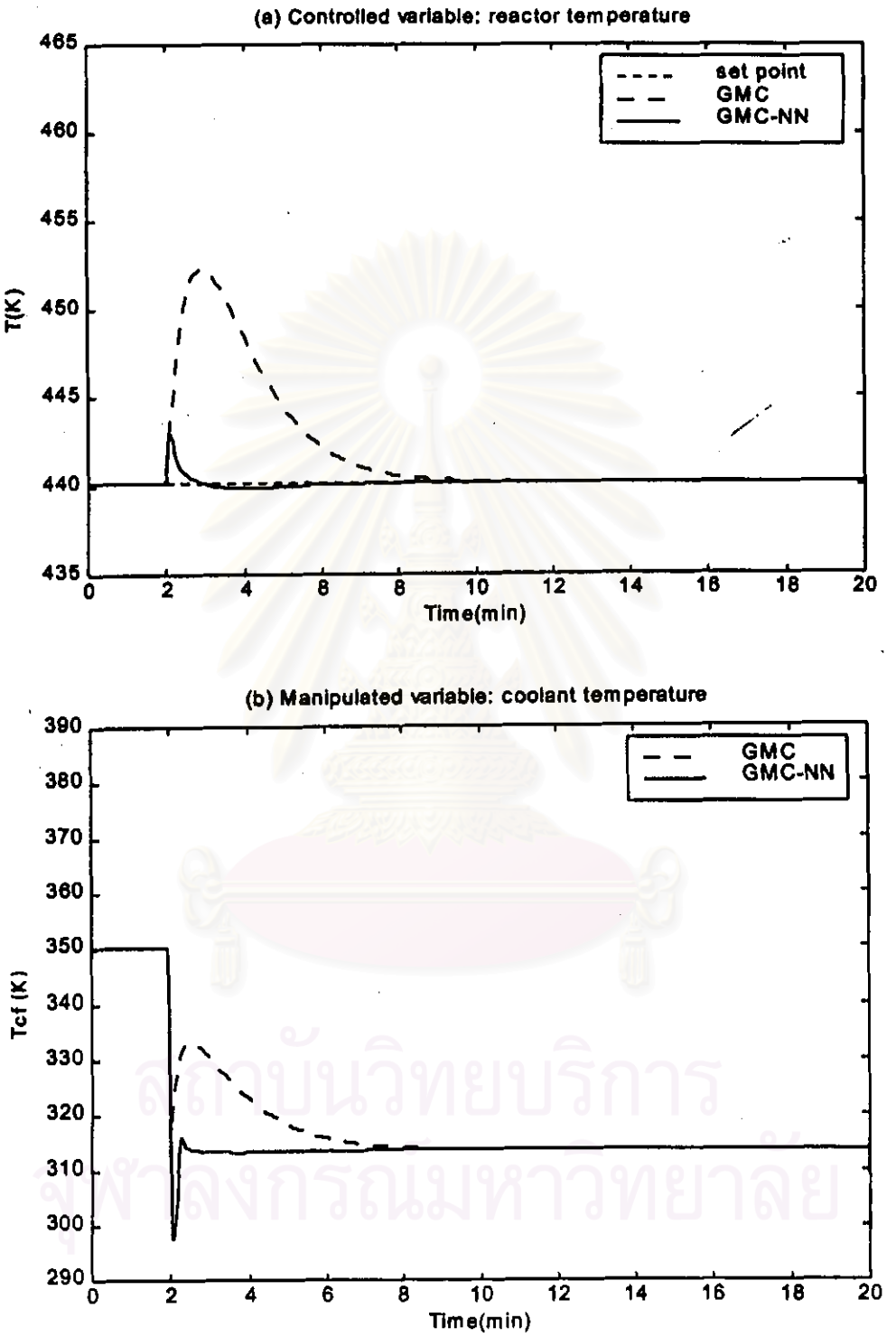

Figure 6.8: Disturbance rejection and robustness tests with GMC and GMC-NN. Response to 10% load disturbance in the measured feed temperature and 20% model error in the pre-exponential constant

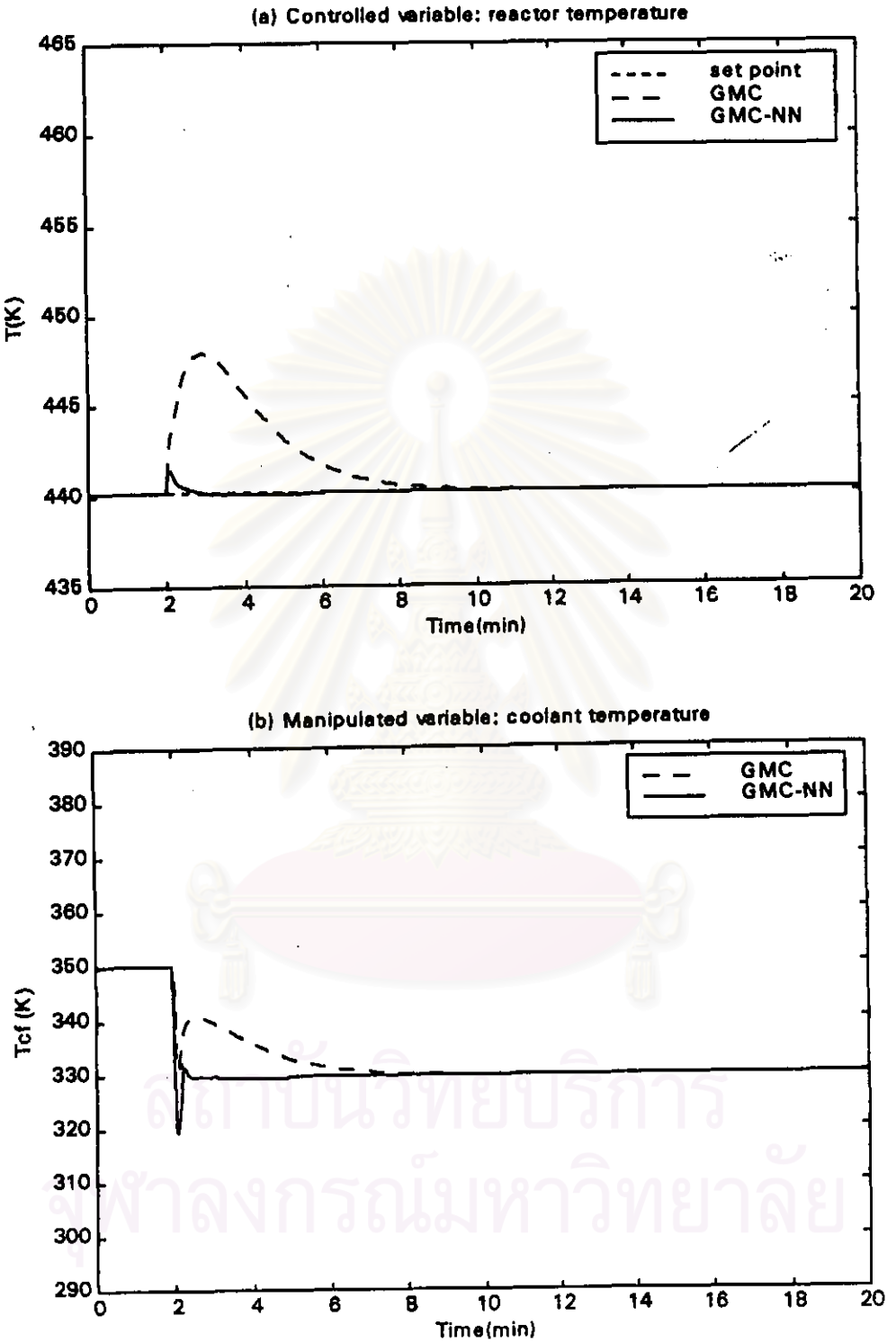

Figure 6.9: Disturbance rejection and robustness tests with GMC and GMC-NN. Response to 10% load disturbance in the unmeasured feed concentration and 20% model error in the pre-exponential constant

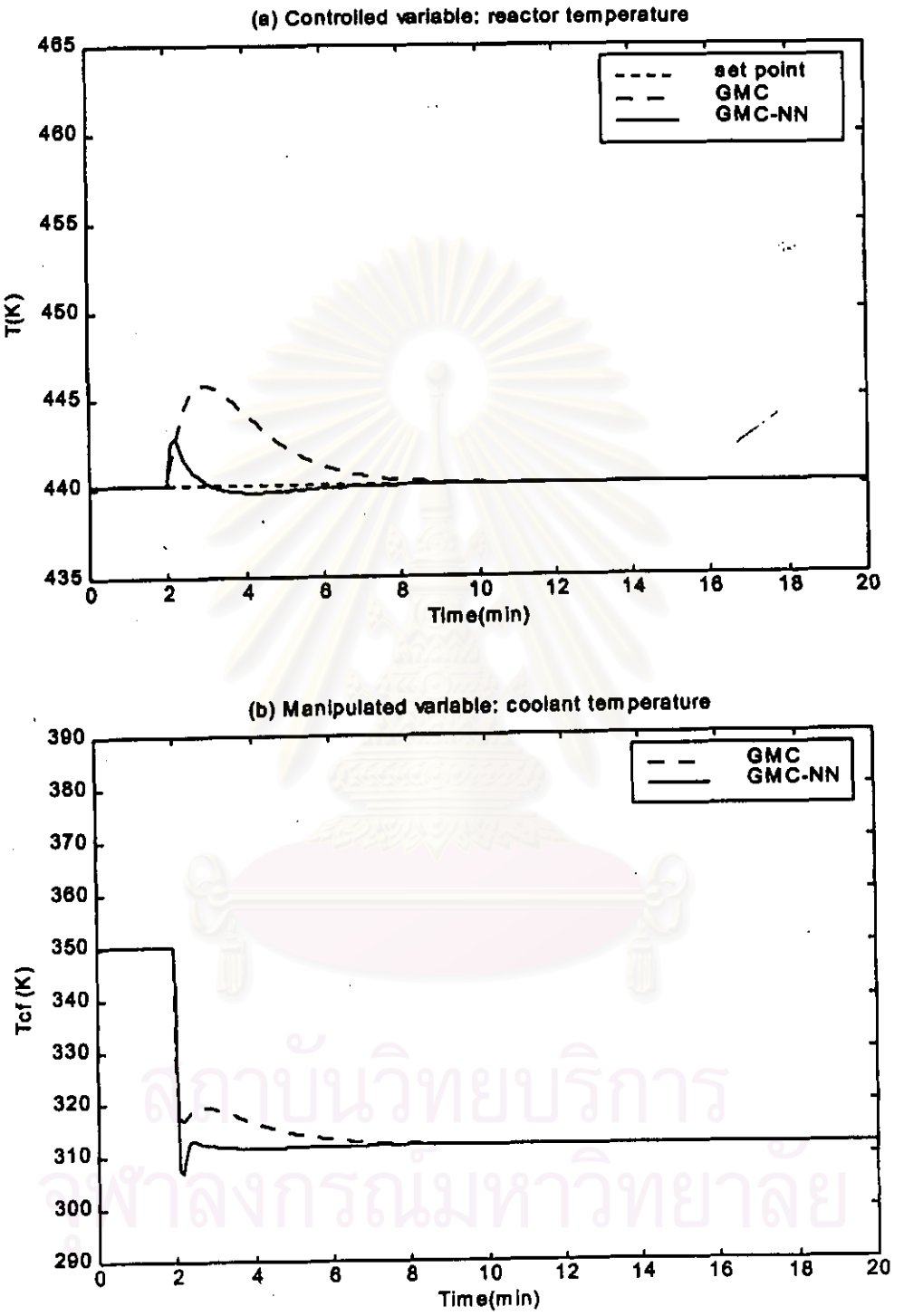

Figure 6.10: Disturbance rejection and robustness tests with GMC and GMC-NN. Response to 10% load disturbance in the measured feed temperature and -50% model error in the heat transfer coefficient

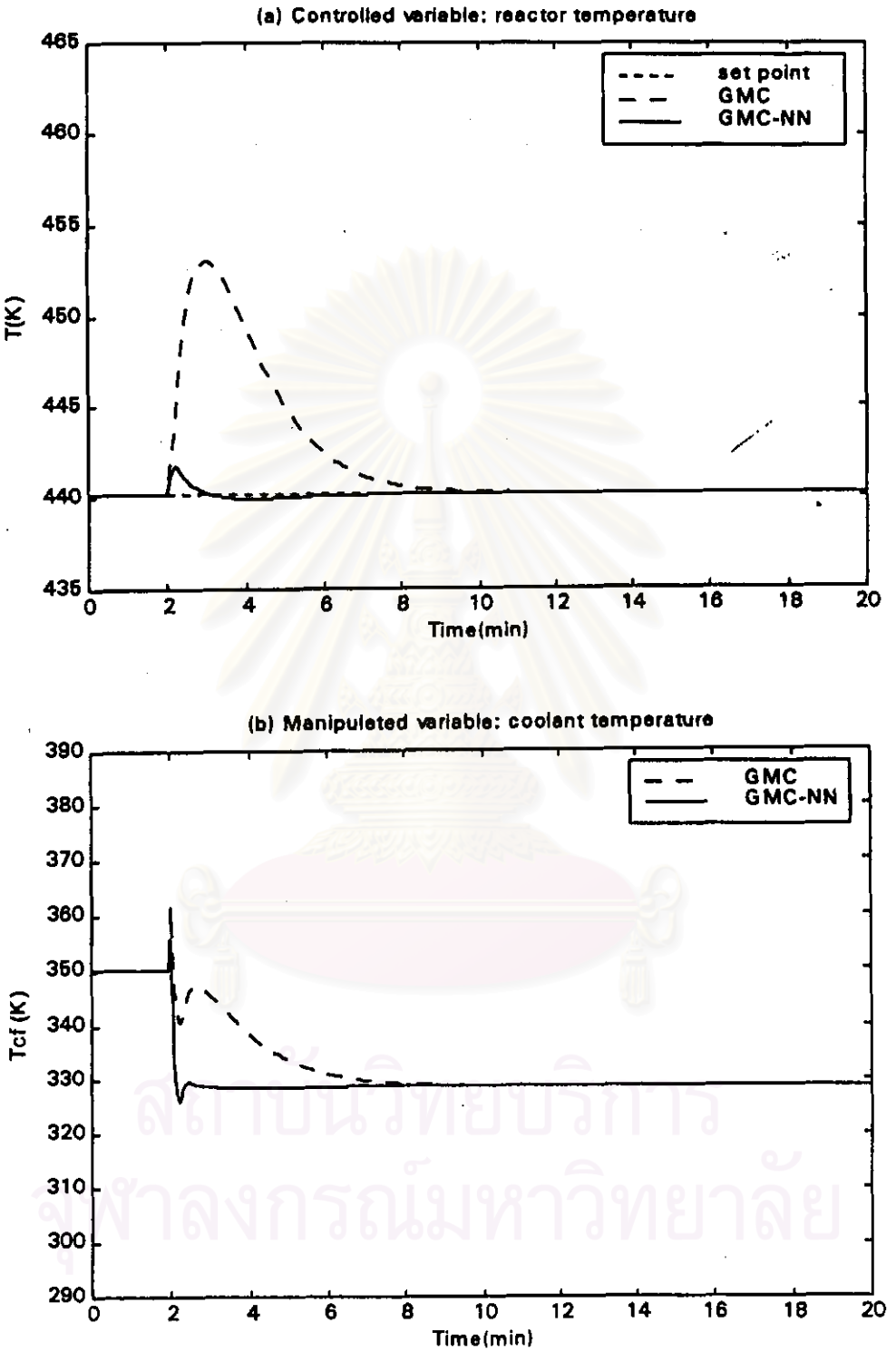

Figure 6.11: Disturbance rejection and robustness tests with GMC and GMC-NN. Response to 10% load disturbance in the unmeasured feed concentration and -50% model error in the heat transfer coefficient

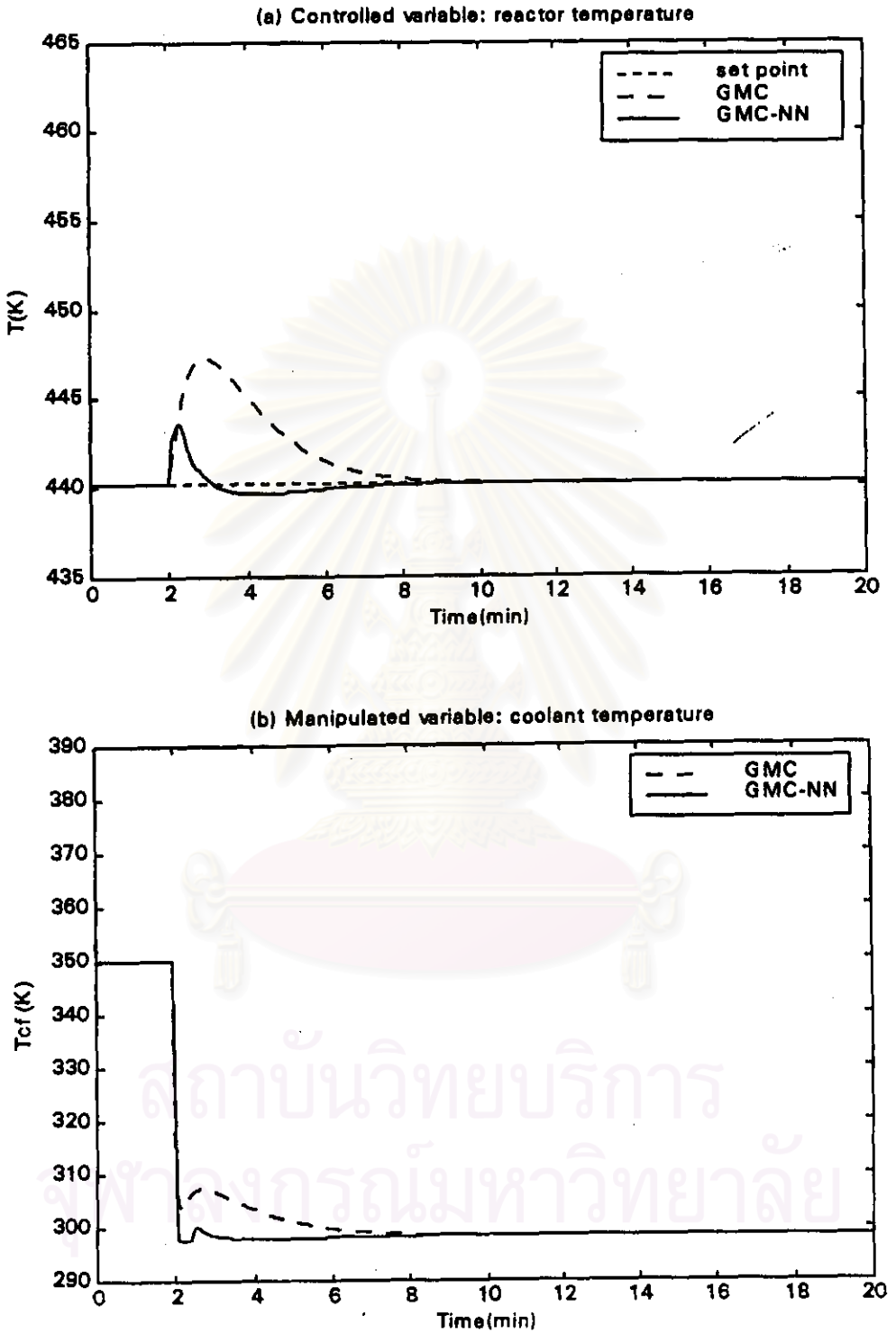

Figure 6.12: Disturbance rejection and robustness tests with GMC and GMC-NN. Response to 10% load disturbance in the measured feed temperature and 10% model error in the heat of reaction

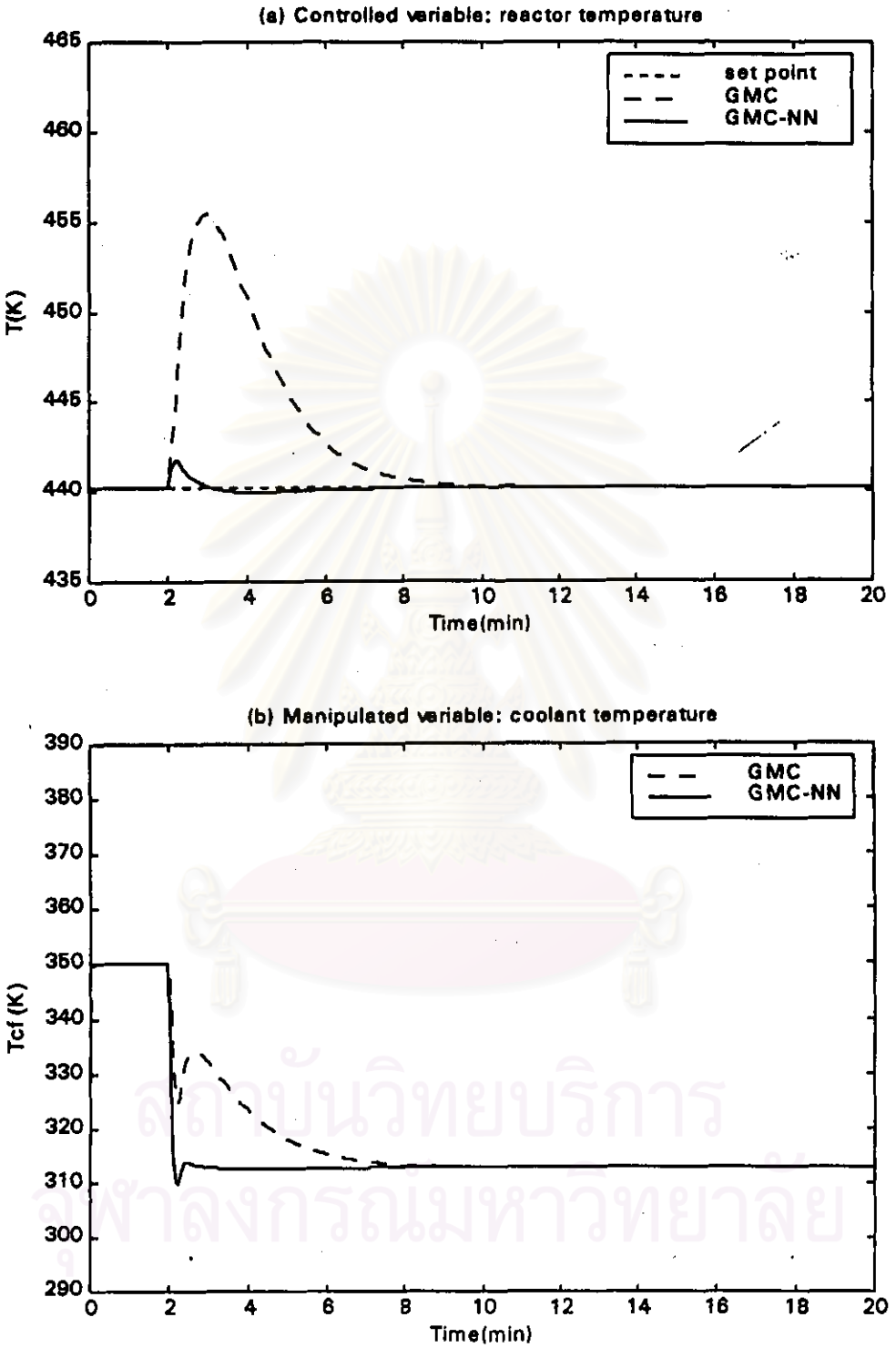

Figure 6.13: Disturbance rejection and robustness tests with GMC and GMC-NN. Response to 10% load disturbance in the unmeasured feed concentration and 10% model error in the heat of reaction

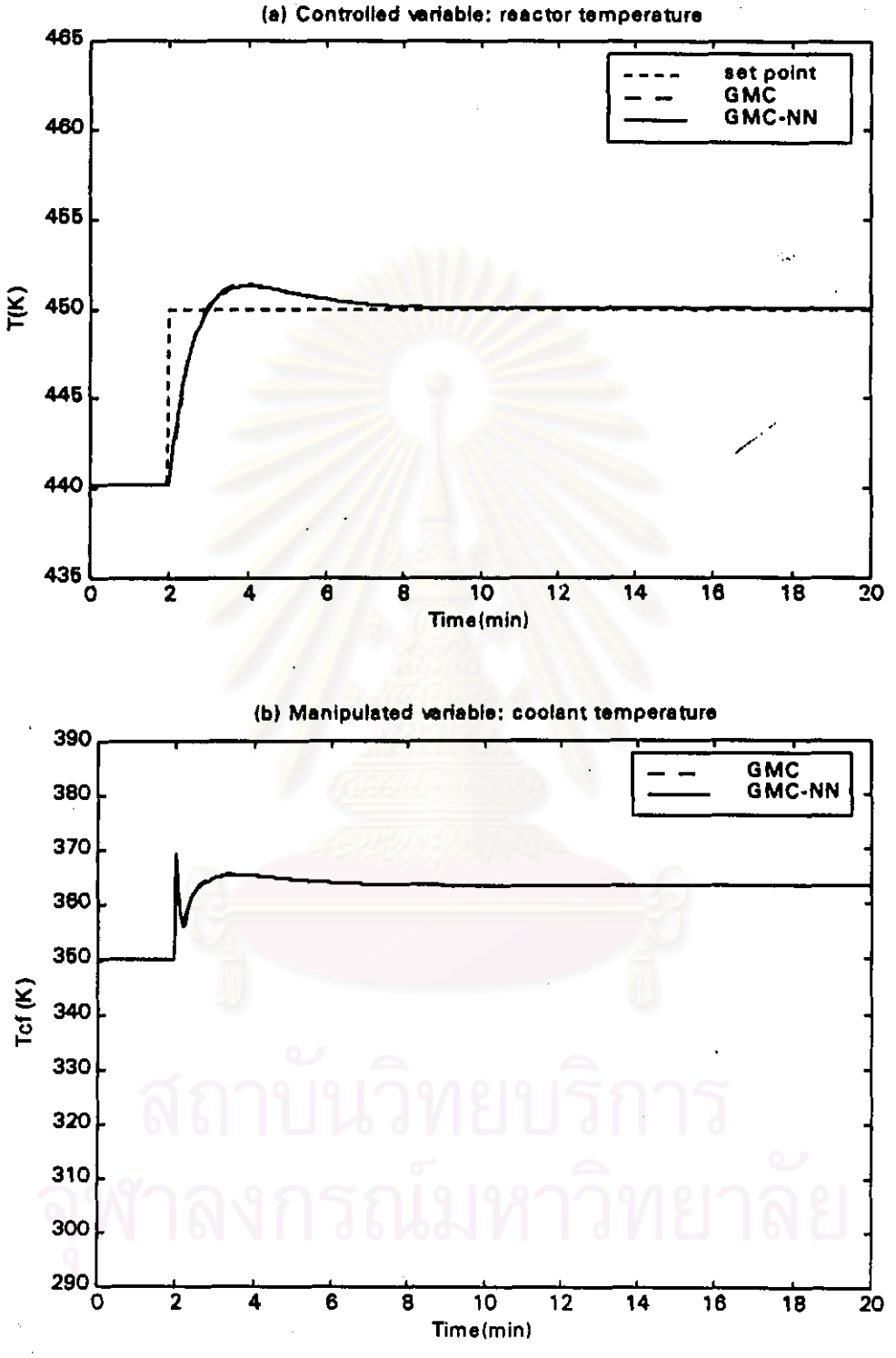

Figure 6.14: Set point tracking test with GMC and GMC-NN.
Set pint change from 440.2 K to 450 K

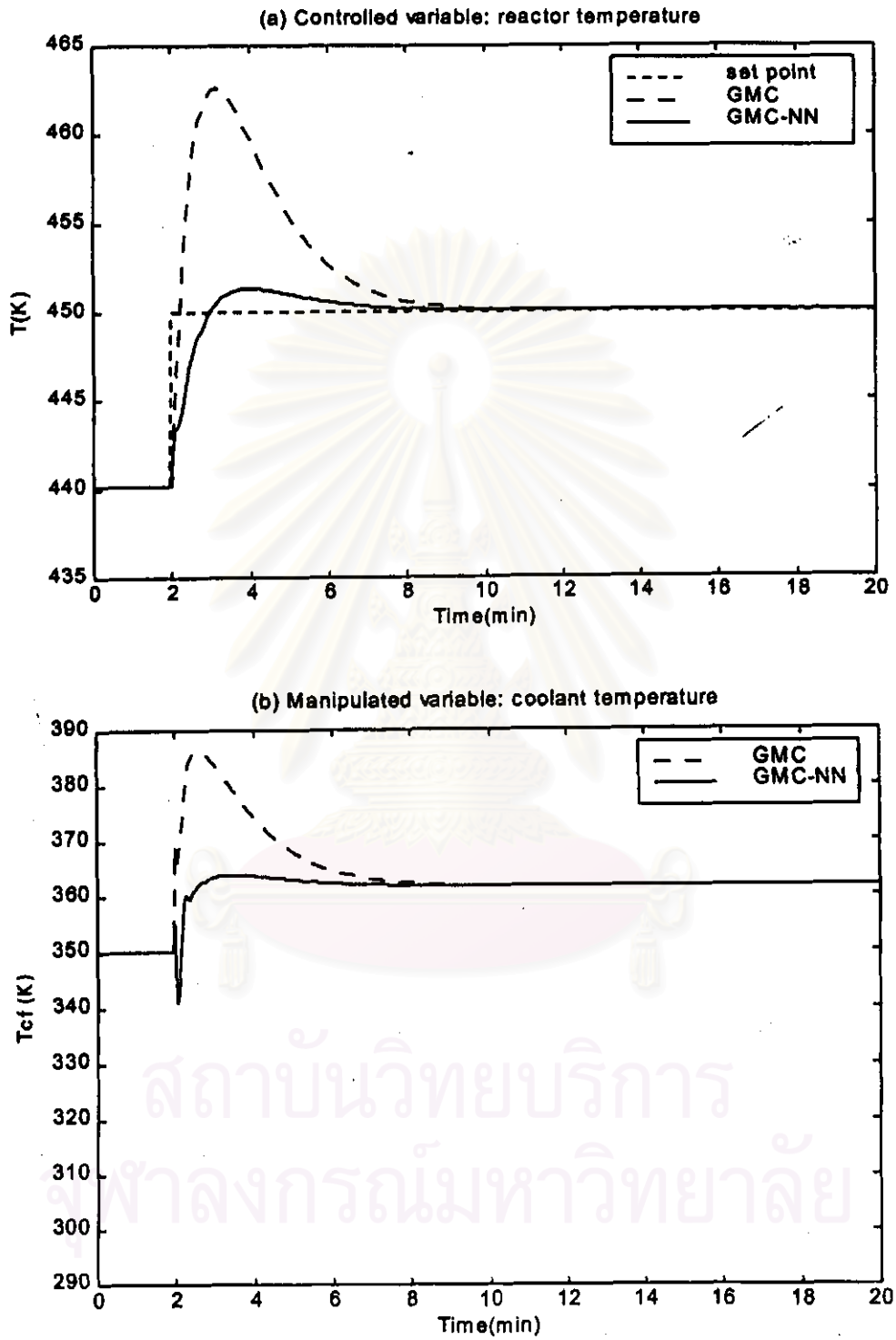

Figure 6.15: Set point tracking and robustness tests with GMC and GMC-NN.
Set point changes from 440.2 K to 450 K and
20% model error in the pre-exponential

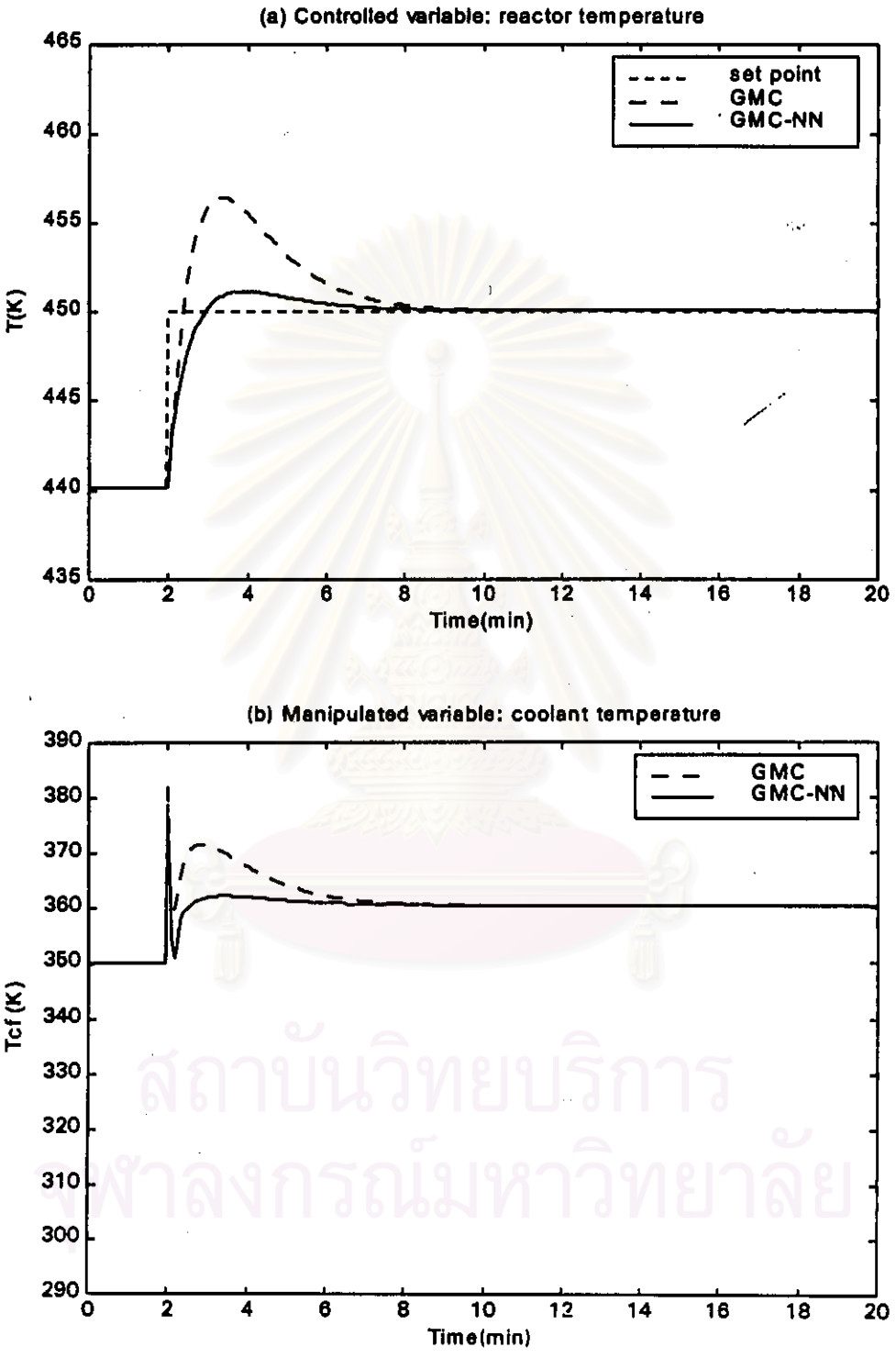

Figure 6.16: Set point tracking and robustness tests with GMC and GMC-NN.
Response to set point changes from 440.2 K to 450 K and
–50% model error in heat transfer coefficient

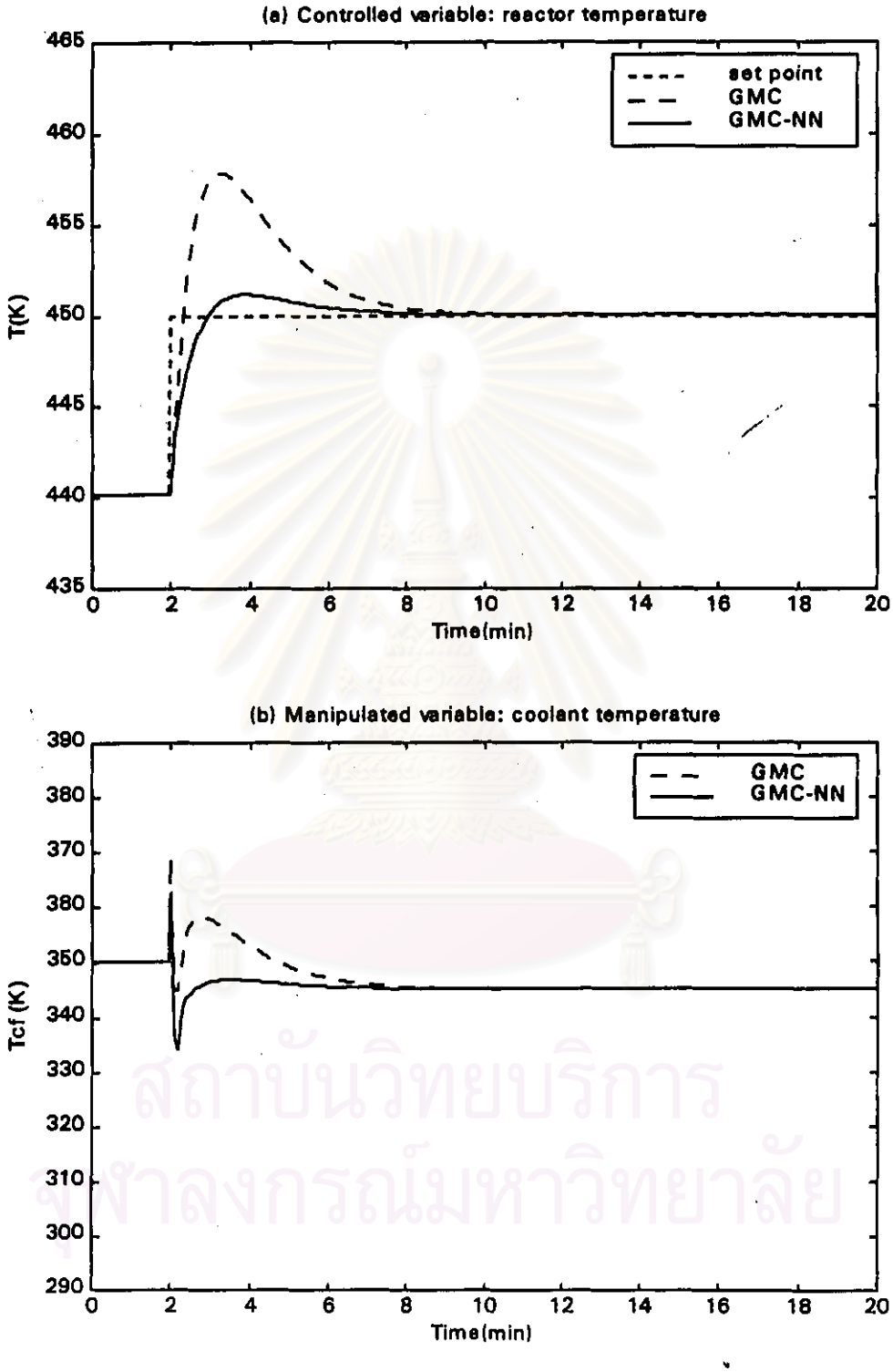

Figure 6.17: Set point tracking performance test with GMC and GMC-NN.
Response to set point change from 440.2 K to 450 K and
10% model error in heat of reaction

6.4 Results and Discussions

The control performance of the GMC with neural network approximator (GMC-NN) for reactor temperature control is compared with that of GMC with a state estimator derived from the mass balance. Both control performances are evaluated with disturbance rejection and set point tracking in nominal condition; parameters are not changed and in the presence of plant-model mismatches as given in Table 6.2. All changes of the disturbances, set point, and parameters studied in this work result in the increase of the reactor temperature. Consequently, the coolant feed temperature has to be reduced so that the reactor temperature can be brought back its desired set point.

The disturbance rejection tests consist of 10% change of feed temperature and 10% change of feed concentration from their nominal values. With 10% change of feed temperature in nominal condition, it was found that the GMC with the state estimator can lead to very good control performance, that is, the system is controlled closely to its set point while small overshoot happens in GMC-NN configuration as depicted in Figure 6.6. This may be caused from the reason that the feed temperature is available online and no plant/model mismatch exists, therefore the state estimator produces the correct value of concentration. As the results, the GMC with the state estimator gives a better control performance than GMC-NN. Moreover, neural network approximator is a black-box model generating the function f based on the coolant and the reactor temperature. Thus, some model errors are included in the function approximation. However, the GMC-NN control configuration is able to control the reactor temperature closely to its set point when the system is disturbed with 10% change of feed concentration but some overshoots occur in GMC with state estimator as shown in Figure 6.7.

In the presence of plant-model mismatches, the GMC-NN can control the reactor temperature at its set point with smaller overshoot compared with the GMC with the state estimator as shown in Figure 6.8 to Figure 6.13.

In case of the plant/model mismatch in the Arrhenius pre-exponential constant, the GMC-NN can control the reactor temperature at its set point with smaller overshoot than in the result obtained from the GMC with the state estimator as illustrated in Figure 6.8 and Figure 6.9. Additionally, both control configurations give larger overshoots when the system is disturbed by the change in feed temperature than when disturbed by the change in the feed concentration. This can be implied that the disturbance of the feed temperature affects the system more than that of the feed concentration when the plant-model mismatch in the Arrhenius pre-exponential constant happens.

In case of the plant/model mismatch in the heat transfer coefficient, the change in the feed temperature has less effect to the system than in the feed concentration as demonstrated in Figure 6.10 and Figure 6.11.

In case of the plant/model mismatch in the heat of reaction, the change in the feed temperature also affects the system less than that in the feed concentration as demonstrated in Figure 6.12 and Figure 6.13.

For the tests with set point tracking, the results obtained from both control configuration in nominal case are equivalent as depicted in Figure 6.14. Nevertheless, large overshoots still exist in plant/model mismatch condition as shown in Figure 6.15, Figure 6.16, and Figure 6.17. It can be concluded that the use of neural networks with the GMC as the hybrid method is able to improve the control performance of the GMC as well.

Conclusively, the GMC-NN configuration can reject either measured disturbances or unmeasured disturbances, which affect the increase of the reactor temperature in both nominal condition and plant-model mismatch condition. However, the GMC with state estimator indicates better control performance than the GMC-NN when the system is disturbed with measured disturbance in nominal condition. In case of the set point tracking test, the control performances of both control configurations are equivalent when the system is tested in nominal condition. With the set point tracking test in plant/model

mismatch condition, the GMC-NN can lead the reactor temperature back to its set point with smaller overshoot than that of GMC with state estimator.